Human replicative DNA polymerase δ can bypass T-T (6-4) ultraviolet photoproducts on template strands

Takeo Narita[1], Toshiki Tsurimoto[2], Junpei Yamamoto[3], Kana Nishihara[1], Kaori Ogawa[2], Eiji Ohashi[2], Terry Evans[1], Shigenori Iwai[3], Shunichi Takeda[1] and Kouji Hirota[1]*

[1]*Department of Radiation Genetics, Graduate School of Medicine, Kyoto University, Yoshidakonoe, Sakyo-ku, Kyoto 606-8501, Japan*
[2]*Department of Biology, School of Sciences, Kyushu University, 6-10-1 Hakozaki, Higashi-ku, Fukuoka 812-8581, Japan*
[3]*Division of Chemistry, Graduate School of Engineering Science, Osaka University, 1-3 Machikaneyama, Toyonaka, Osaka 560-8531, Japan*

DNA polymerase δ (Polδ) carries out DNA replication with extremely high accuracy. This great fidelity primarily depends on the efficient exclusion of incorrect base pairs from the active site of the polymerase domain. In addition, the 3′–5′ exonuclease activity of Polδ further enhances its accuracy by eliminating misincorporated nucleotides. It is believed that these enzymatic properties also inhibit Polδ from inserting nucleotides opposite damaged templates. To test this widely accepted idea, we examined *in vitro* DNA synthesis by human Polδ enzymes proficient and deficient in the exonuclease activity. We chose the UV-induced lesions cyclobutyl pyrimidine dimer (CPD) and 6-4 pyrimidone photoproduct (6-4 PP) as damaged templates. 6-4 PP represents the most formidable challenge to DNA replication, and no single eukaryotic DNA polymerase has been shown to bypass 6-4 PP *in vitro*. Unexpectedly, we found that Polδ can perform DNA synthesis across both 6-4 PP and CPD even with a physiological concentration of deoxyribonucleotide triphosphates (dNTPs). DNA synthesis across 6-4 PP was often accompanied by a nucleotide deletion and was highly mutagenic. This unexpected enzymatic property of Polδ in the bypass of UV photoproducts challenges the received notion that the accuracy of Polδ prevents bypassing damaged templates.

Introduction

Polδ is involved in lagging strand DNA replication and excision repair pathways (Blank *et al.* 1994; Burgers 1998; Kunkel & Burgers 2008; Nick McElhinny *et al.* 2008). Polδ consists of four subunits – p125, p50, p66 and p12 (Podust *et al.* 2002). The catalytic p125 subunit and the p50 subunit are highly conserved among eukaryotic species and are essential for cell proliferation. In addition to the polymerase domain, the p125 subunit contains a 3′–5′ exonuclease domain, which is responsible for its proofreading activity. In association with PCNA, Polδ is highly processive and synthesizes DNA with remarkable accuracy, catalyzing approximately one error per 10^6 nucleotides polymerized *in vivo*. This exceptional accuracy is achieved by the following two enzymatic properties of Polδ: (i) Polδ discriminates accurately between correct and incorrect base pairs at the polymerase active site. This is achieved by the spatially constrained polymerase active site that accommodates only correct base pairs (Yang 2005; Burgers 2009). (ii) Proofreading, achieved by the exonuclease activity of Polδ, further increases the accuracy by 10–60-fold (Fortune *et al.* 2005). With respect to replication of damaged templates, these enzymatic properties are suggested to inhibit Polδ from bypassing lesions in the following ways. The accurate discrimination of Polδ prevents the incorporation of any nucleotide opposite damaged bases, because the comparatively small active site of Polδ does not permit base pairing involving damaged bases. Furthermore, even after nucleotides are inserted opposite damaged bases, they are eliminated by the proofreading activity of Polδ because a base pair involving a damaged nucleotide

Communicated by: Hiroyuki Araki
**Correspondence*: khirota@rg.med.kyoto-u.ac.jp

DOI: 10.1111/j.1365-2443.2010.01457.x

does not conform to canonical Watson–Crick geometry. Therefore, it is believed that Polδ is incapable of bypassing damaged templates.

UV light induces two major UV photoproducts on genomic DNA, CPD and 6-4 PP. These UV lesions stall replicative DNA polymerases *in vivo* and significantly delay the elongation of newly synthesized DNA (Prakash 1981; Edmunds *et al.* 2008; Guo *et al.* 2008; Niimi *et al.* 2008). Compared with CPD, 6-4 PP introduces stronger structural distortions into the DNA backbone, leading to a much tougher block to replication (Kim & Choi 1995). To release such replication blockage, cells mobilize specialized DNA polymerases, translesion synthesis (TLS) polymerases, which insert nucleotides opposite UV photoproducts and further extend DNA synthesis (Friedberg *et al.* 2005; Lehmann *et al.* 2007; Guo *et al.* 2009). The current model for TLS is that stalled replicative polymerases at the damaged template strands are replaced by specialized TLS polymerases, including Polζ and Polη. Consistent with stronger DNA distortion introduced by 6-4 PP than by CPD, no single eukaryotic polymerase is able to bypass 6-4 PP, whereas Polη alone performs bypass synthesis across CPD (McCulloch *et al.* 2004; Friedberg *et al.* 2005).

The capability of TLS polymerases to bypass DNA damage is attributable to their three-dimensional structures, which differs from that of replicative polymerases. The active site of TLS polymerases is larger and is thus able to accommodate DNA lesions and incorrect base pairings (Ling *et al.* 2001; Silvian *et al.* 2001; Trincao *et al.* 2001; Yang 2005; Wang & Yang 2009). As a consequence, TLS polymerases undergo DNA synthesis with limited accuracy, and flexibly insert nucleotides opposite damaged bases, and can also extend DNA synthesis from a primer with a mismatch at its 3′ end (Lehmann *et al.* 2007; Guo *et al.* 2009; Waters *et al.* 2009). Nonetheless, it should be noted that this extension step is a challenge for all DNA polymerases, because the polymerase activity is inhibited by the abnormal structure of the primer/template duplex, caused by a mismatch. Consistent with this, in the bypass of T-T UV damage, TLS polymerases incorporate the first base opposite the 3′ T of a thymidine dimer more efficiently than the second base opposite the 5′ T, because the second incorporation is an extension from the primer's 3′ end, which does not properly hybridize with the 3′ T of UV damage (Meng *et al.* 2009).

In a separate study to analyze the function of the Polδ p66 component, we generated *polδ p66*$^{-/-}$ cells from the chicken DT40 B-cell line. Remarkably, *polδ p66*$^{-/-}$ cells can proliferate and undergo replication with a normal rate (manuscript in preparation). Interestingly, however, *polδ p66*$^{-/-}$ cells exhibited hypersensitivity to a wide variety of DNA-damaging agents, including UV. This hypersensitivity is attributable to impaired TLS across UV photoproducts, raising the possibility that Polδ might be able to undergo TLS. To test this hypothesis, in this study, we analyzed the capability of purified human Polδ to bypass CPD- and 6-4 PP-containing oligonucleotide templates. Surprisingly, even wild-type Polδ [Polδ (wt)] possessing the exonuclease activity was able to bypass 6-4 PP. As this nuclease activity eliminates the nucleotides incorporated opposite damaged templates, we may have underestimated the efficiency of inserting nucleotides opposite UV lesions by Polδ. To accurately measure this efficiency, we purified Polδ (exo-) that carries a point mutation in conserved exonuclease domain. We here characterize this novel and unique enzymatic property of Polδ in bypassing 6-4 PP as well as CPD.

Results

Polδ incorporates nucleotides opposite UV photoproducts

We analyzed the capability of Polδ to undergo DNA synthesis across CPD and 6-4 PP. To this end, we simultaneously expressed the four human Polδ subunits (p125, p66, p50 and p12) in insect cells and purified Polδ holoenzyme [Polδ (wt)] to near homogeneity (Fig. 1, Fig. S1 in Supporting Information). We used this enzyme for *in vitro* primer extension assays using a 30mer oligonucleotide template containing a single CPD or 6-4 PP (Fig. 1). We used Polη as a positive control, because previous studies have shown that Polη readily bypasses CPD with high efficiency (Masutani *et al.* 1999a,b, 2000; McCulloch *et al.* 2004), whereas it incorporates only one or two bases opposite 6-4 PP without appreciable extension (Yamamoto *et al.* 2008). This experiment was carried out in the presence of 100 μM dNTPs as previously reported, which is ten times higher than the physiological concentration of dNTPs *in vivo* (Traut 1994). We confirmed that Polη indeed bypassed CPD efficiently, whereas it incorporated only one base opposite the 6-4 PP lesion with very poor extension (McCulloch *et al.* 2004) (Fig. 2).

We also examined the capability of Polδ to bypass DNA lesions with 100 μM dNTPs, as it has been shown that Polδ can bypass abasic sites under this con-

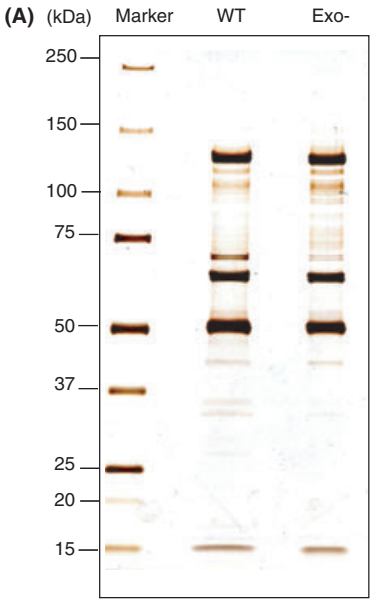

(B)

Primers

16mer primer	5′-CACTGACTGTATGATG-3′
17mer primer	5′-CACTGACTGTATGATGA-3′
polyT primer	5′-TTTTTTTTTTTTTTTTTTTT-3′

Template

30mer normal template	5′-CTCGTCAGCATCTTCATCATACAGTCAGTG-3′
30mer CPD template	5′-CTCGTCAGCATC<u>TT</u>CATCATACAGTCAGTG-3′
30mer 6-4PP ATC template	5′-CTCGTCAGCATC<u>TT</u>CATCATACAGTCAGTG-3′
30mer 6-4PP AAT template	5′-CTCGTCAGCAAT<u>TT</u>CATCATACAGTCAGTG-3′
30mer 6-4PP TAC template	5′-CTCGTCAGCTAC<u>TT</u>CATCATACAGTCAGTG-3′
30mer 6-4PP AAC template	5′-CTCGTCAGCAAC<u>TT</u>CATCATACAGTCAGTG-3′

ssDNA to measure exonuclease activity

51mer ssDNA	5′-TTTTTTTTTTTTTTTTTTTTTTTTTTTTTACGACGTTGTAAAAGGACGGGCCAGT-3′

Figure 1 Purified human Polδ wild-type and exonuclease-mutant holoenzymes and oligonucleotides used in this study. (A) Expression and purification of recombinant human Polδ. Purified Polδ wild-type (wt) and exonuclease-mutant enzymes (exo-) were electrophoresed in an SDS 12.5% polyacrylamide gel and stained using silverstaining kit (Wako). (B) Sequences of oligonucleotide primers and templates used in this study. The 16mer primer, 17mer primer and 30mer templates were used in the primer extension assay. Cyclobutyl pyrimidine dimers (CPD) and (6-4) pyrimidone photoproducts were incorporated at the underlined site in the lesion template. The 51mer ssDNA was labeled with biotin at the 5′ end and used to examine the exonuclease activity of Polδ.

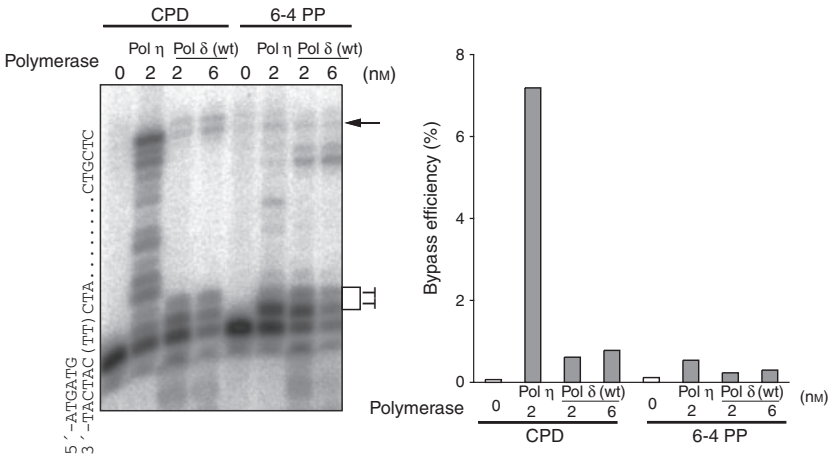

Figure 2 Polδ bypasses the UV photoproducts CPD and 6-4 PP at a high dNTP concentration. Gel image showing DNA synthesis across CPD and 6-4 PP (left panel). The indicated concentration (2 and 6 nM) of Polδ (wt) or 2 nM Polη (control) was incubated with 8 nM of the primer/template substrate for 15 min in the presence of 100 μM dNTPs as described in Experimental procedures. Parentheses indicate the position of T-T dimer on the template. The position of the fully elongated product is indicated with an arrow. The graph shows the quantitative data of synthesis efficiency on an damaged template (right panel). We quantified the intensity of the bands corresponding to the full-length product and unextended primer. Synthesis efficiency was calculated using the following formula: intensity of the full-length band/intensity of the unextended primer.

dition (Fazlieva *et al.* 2009; Meng *et al.* 2009). As previously reported, the purified Polδ did bypass the abasic site (Fig. S1 in Supporting Information), verifying the functionality of our recombinant proteins. Next, we used a CPD lesion-containing template and observed the generation of fully elongated products (30mer

products as well as 31mer products, representing a 1-bp extension) as well as the intermediate products of TLS, where only one or two bases were inserted opposite the CPD. The amount of fully elongated products was approximately 0.7% of the primer used (Fig. S2 in Supporting Information). This result was again consistent with previous reports that showed that <1% of CPD lesions were bypassed efficiently by Polδ.

We tested the 6-4 PP lesion-carrying template, which is heavily distorted and therefore thought to be considerably more difficult to bypass than abasic sites or CPD lesions. To our surprise, Polδ (wt) also incorporated one or two bases opposite 6-4 PP (Fig. 2) and was even able to generate fully elongated products (Fig. 2). We therefore conclude that 6-4 PP does not completely inhibit *in vitro* DNA synthesis by Polδ; indeed, we may have underestimated the amount of incorporated nucleotides opposite the UV photoproduct because a substantial fraction of these may be removed by the proofreading activity of Polδ.

Characterization of exonuclease-deficient Polδ mutant

To more accurately measure Polδ-dependent DNA synthesis over the UV photoproducts, we purified mutant Polδ deficient in 3′–5′ exonuclease activity [Polδ (exo-)]. To this end, we replaced the conserved Asp402 residue of the exonuclease domain with Ala. The yield of purified Polδ (exo-) holoenzyme was the same as intact Polδ (wt) (Fig. 1), indicating that the mis-sense mutation did not affect protein stability. We evaluated the 3′–5′ exonuclease activity by incubating purified Polδ with a 5′ biotin-labeled single-strand (ss) oligonucleotide (Figs 1 and 3). As expected, Polδ (wt) digested this ssDNA in a dose-dependent manner, whereas Polδ (exo-) showed no detectable nuclease activity (Fig. 3).

It is known that the dNTP concentration affects the 3′–5′ exonuclease activity of some DNA polymerases (Brutlag & Kornberg 1972). To investigate this issue in our system, we incubated Polδ (wt) and the 5′ end labeled ssDNA with various concentrations of dNTPs and measured the digestion of this ssDNA. Without dNTPs, more than half of the primer was degraded (Fig. 3). In contrast, the addition of dNTPs suppressed the degradation of the ssDNA substrate in a dNTP concentration-dependent manner (Fig. 3). We therefore conclude that the exonuclease activity is indeed considerably suppressed by dNTPs.

We subsequently analyzed *in vitro* DNA synthesis with a physiological dNTP concentration of 10 μM,

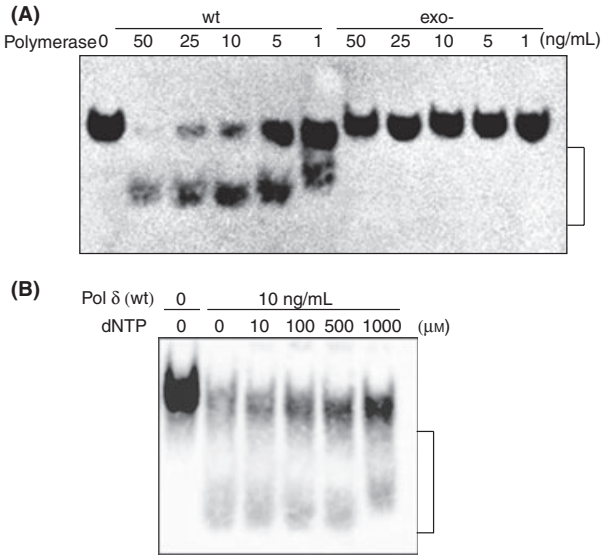

Figure 3 Impaired exonuclease activity of Polδ by substitution of Asp 402 with Ala in the Polδ p125 catalytic subunit. (A) Exonuclease activity of Polδ (wt) and Polδ (exo-) holoenzymes. A concentration of 0.5 μM of biotin-labeled 51mer ssDNA (Fig. 1) was incubated with sequentially diluted polymerases (1–50 ng/mL) at 37 °C for 15 min. The reaction was terminated by adding 1 μL of loading buffer (Takara) and analyzed with 7.5% polyacrylamide gel as described in Experimental procedures. Open parenthesis represents the degraded product. (B) dNTPs suppress the exonuclease activity of Polδ. Exonuclease activity of Polδ (wt) in the presence of 10, 100, 500 and 1000 nM dNTPs. A concentration of 10 ng/mL Polδ was incubated with 30 fmol of biotin-labeled 51mer ssDNA in the presence of the indicated concentration of dNTPs. Open parenthesis represents the degraded product.

which is observed in cycling human cells (0.4–17 μM) (Jamburuthugoda *et al.* 2006). By evaluating the efficiency of DNA synthesis on undamaged template DNA strands by measuring the amount of fully elongated products, we demonstrated that Polδ (exo-) showed higher efficiency of DNA synthesis compared with Polδ (wt). Loss of the exonuclease activity might suppress the digestion of synthesized DNA and thereby leads to the augment of *in vitro* DNA synthesis product (Fig. 4A,B).

Loss of the 3′–5′ exonuclease activity increased the capability of Polδ to carry out TLS across CPD and 6-4 PP

To measure the inhibitory effect of Polδ's proofreading activity on TLS, we compared the DNA synthesis by Polδ (wt) and Polδ (exo-) on lesion-containing

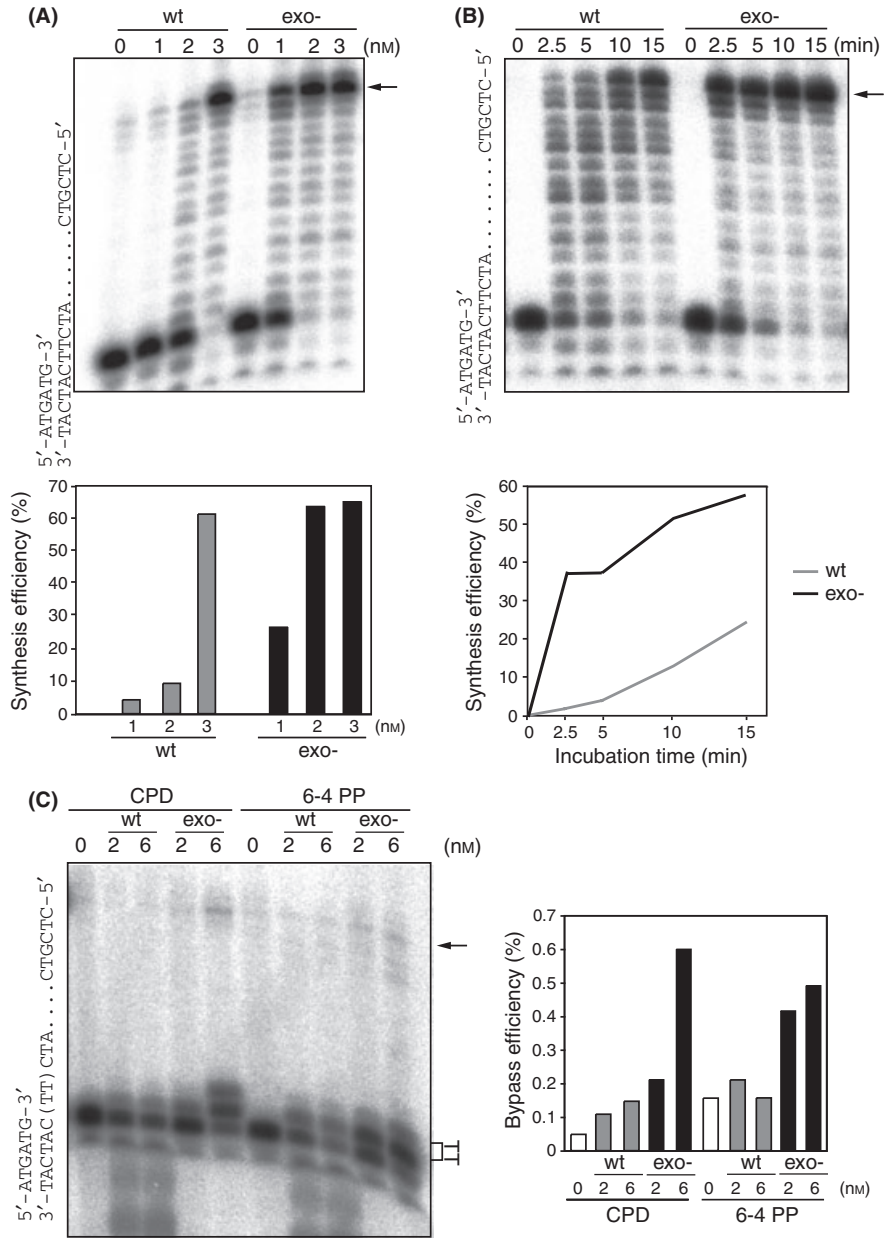

Figure 4 Polδ (exo-) bypasses CPD and 6-4 PP at a physiological dNTP concentration. (A) Gel image showing DNA synthesis of varying concentration of Polδ on an undamaged template. The indicated concentration (0, 1, 2 and 3 nM) of Polδ (wt or exo-) was incubated in a 5 μL reaction mix containing 10 μM dNTPs and 8 nM of the primer/template substrate for 15 min as described in Experimental procedures. The graph shows the quantitative data of synthesis efficiency on an undamaged template. Synthesis efficiency was calculated as described in Fig. 2. (B) Time-course analysis of DNA synthesis by Polδ (wt) and Polδ (exo-). Two nanomolar of Polδ (wt or exo-) was incubated in a 50-μL reaction mixture containing 10 μM dNTPs with 8 nM of the primer/template substrate. In the indicated time point, reaction was terminated. The graph shows the quantitative data of synthesis efficiency on an undamaged template as in panel A. (C) Gel image showing DNA synthesis across CPD and 6-4 PP (left panel). DNA synthesis reactions across CPD or 6-4 PP were carried out with the indicated concentration (2 and 6 nM) of Polδ (wt or exo-) for 15 min in a 5-μL reaction mixture containing 10 μM dNTPs and 8 nM of the primer/template substrate. Parentheses indicate the position of T-T dimer on the template. The position of the fully elongated product is indicated with an arrow. The graph shows the quantitative data of synthesis efficiency on an damaged template (right panel). Synthesis efficiency was calculated as described in Fig. 2.

templates. With 10 μM dNTPs, Polδ (wt) stalled after the incorporation of only a single base, probably opposite the 3′ T of CPD or 6-4 PP (Fig. 4C). At this physiological dNTP concentration, the efficiency of Polδ-dependent TLS across CPD and 6-4 PP was significantly reduced compared to TLS with 100 μM dNTPs (compare Figs 2 and 4C). As expected, the amount of the unextended radio-labeled primer was significantly increased after incubation with Polδ (exo-) than after incubation with Polδ (wt), indicating that the primer may have been digested by the exonuclease activity of Polδ (wt). Remarkably, we reproducibly detected a weak but significant band corresponding to fully elongated products even when we used the damage-containing templates. Taken together, with 10 μM dNTPs, Polδ (exo-) is able to fully extend DNA synthesis, whereas Polδ (wt) can insert only a single nucleotide opposite the 5′ T of 6-4 PP.

Analysis of Polδ (exo-)-dependent bypass products across CPD and 6-4 PP

We next analyzed the nucleotide sequences of TLS products generated by Polδ (exo-). To obtain sufficient amounts of TLS products for cloning from the *in vitro* synthesis reaction, we increased the dNTP concentration to 100 μM. On both 6-4 PP- and CPD-containing templates, Polδ (exo-) produced significant amounts of full-length products, containing 30 and 31 nucleotides (Fig. 5A,B). The 31-nucleotide product may be generated by a one-nucleotide addition to the 30-nucleotide product by the terminal transferase activity of Polδ (exo-), because this activity is shared by a number of prokaryotic and eukaryotic DNA polymerases (Clark 1988). In marked contrast to replication of CPD-containing templates, in the primer extension past 6-4 PP, Polδ(exo-) yielded dominant bands corresponding to 27 and 28 nucleotides – 3 nucleotides shorter than the sizes of the fully elongated 30- and 31-nucleotide products (Fig. 5A,B). We assumed that these shorter products were caused by 3-nucleotide slippage events during the bypass of 6-4 PP. The percentage of synthesized products was 14% for 30- and 31-nucleotide products and 21% for 27- and 28-nucleotide ones (Fig. 5B).

To confirm the slippage event, we cloned fully elongated DNA synthesis products and analyzed their nucleotide sequences. To this end, the primer extension reaction was repeated using a biotin-labeled primer annealed to CPD- or 6-4 PP-containing templates. Elongated products were affinity-purified through the interaction between the biotin tag and streptavidin on magnetic beads. Figure 5C shows the nucleotide sequences opposite 5′-CTT-3′ carrying CPD or 6-4 PP. Indeed, more than 80% of the 6-4 PP bypass products contained a 3-nucleotide deletion opposite this UV lesion. This result is consistent with the predominant bands corresponding to 27 and 28 nucleotides (Fig. 5A), which are 3 nucleotides shorter than fully elongated 30- and 31-nucleotide products. We therefore conclude that Polδ (exo-) can bypass 6-4 PP through replication slippage by looping out three nucleotides carrying, including the 6-4 PP lesion.

We also analyzed bypass products of the CPD-containing template strand. Remarkably, 38% of fully elongated products were error-free, whereas 58% of the bypass products carried A to T transversion mutations opposite the 5′ T of CPD (Fig. 5C). Taken together, although Polδ (exo-) is able to efficiently perform DNA synthesis over 6-4 PP and CPD in the presence of 100 μM dNTPs, the fidelity of this replicative polymerase is remarkably limited.

Nucleotides incorporated opposite UV photoproducts by Polδ (exo-)

To measure the preference of nucleotides inserted by Polδ opposite UV photoproducts at a physiological dNTP concentration (10 μM), we performed the *in vitro* nucleotide incorporation assay with each of the four dNTPs separately. The insertion of nucleotides opposite CPD and 6-4 PP is shown in Fig. 6 (upper panel). Consistent with the sequence data of the fully elongated product, Polδ efficiently incorporated only A opposite the 3′ T of CPD (Fig. 6). In contrast, during the bypass of 6-4 PP, whereas incorporation of A was the most efficient, we found that G was also very efficiently incorporated opposite the 3′ T of 6-4 PP (Fig. 6). These preferences are distinct from those of Polι, which displays no such bias (Tissier *et al.* 2000), suggesting that the catalytic center of Polι might be more open than is Polδ, and thereby accommodates the base pairing of any nucleotide with the 3′ T of 6-4 PP.

We next examined the preference of nucleotide insertion after Polδ incorporates A opposite the 3′ T of the UV photoproducts. To this end, we measured the insertion of individual dNTPs using a 17mer primer, which carries an additional A at its 3′ end (Fig. 1). The efficiency of the second nucleotide insertion is shown in Fig. 6 (lower panel). As expected, the overall efficiency of the second

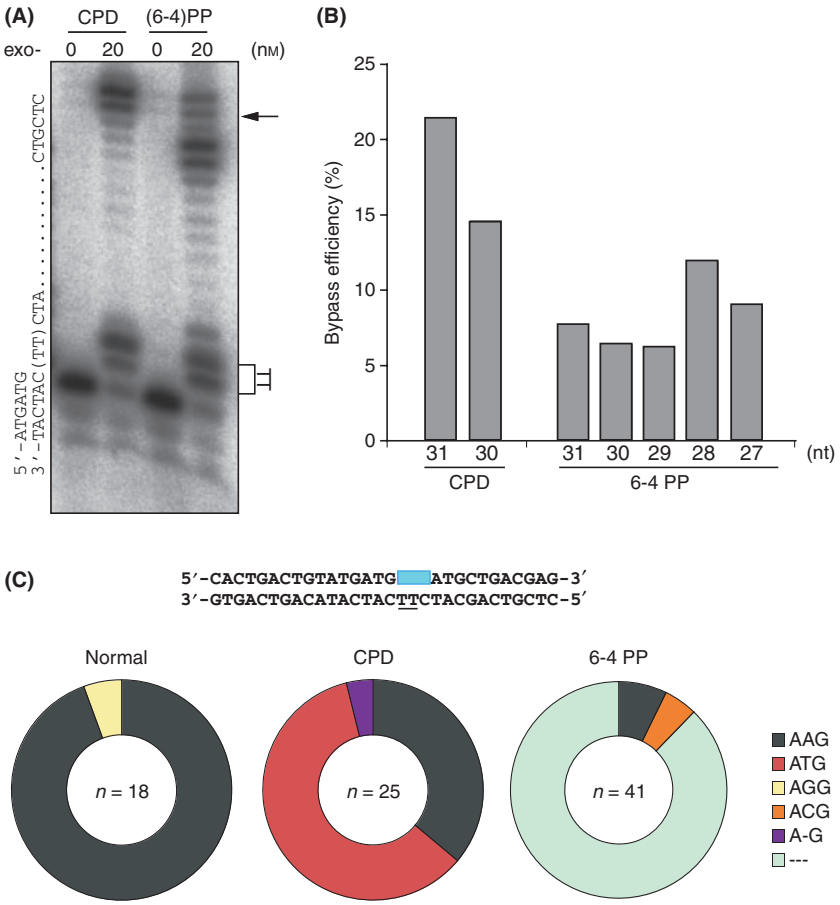

Figure 5 Efficient bypass of Polδ (exo-) holoenzyme across CPD and 6-4 PP at a high dNTP concentration. (A) DNA synthesis reactions across CPD or 6-4 PP. Reactions were carried out at 37 °C with 20 nM Polδ (exo-)-mutant holoenzyme in a 5-μL reaction mixture containing 100 μM dNTPs and 8 nM of the primer/template substrate. Parentheses indicate the position of the T-T dimer on the template. The position of the fully elongated product is indicated with an arrow. Note that the top bands indicate 31mer products, which is 1 nucleotide longer than the template. (B) Quantification of bypass efficiency on damaged templates. The radioactivity of each band was quantified by densitometry. For each product, synthesis efficiency was calculated with the following formula: intensity of the corresponding sized band/the total intensity of all bands. (C) Error-prone bypass of Polδ across CPD and 6-4 PP. Mutation frequencies and mutational spectra focusing on the sequences opposite the 5′-CTT-3′ of the template (the lesion site is underlined). Polδ (exo-) holoenzyme was incubated with the biotin-labeled primers and 100 μM dNTPs. The fully elongated products were purified and sequenced as described in Experimental procedures. All sequence alignment data are shown in Fig. S3 in Supporting Information.

nucleotide insertion was lower than that of the first insertion event (Fig. 6). This limited efficiency of second insertion is probably caused by an abnormal primer/template structure, such as results from mismatched base pairing. We found that Polδ preferentially inserted A and T with a similar efficiency opposite the 5′ T of the UV photoproducts in this second insertion step (Fig. 6). These observations, together with our sequence data (Fig. 5), showed that bypass across UV photoproducts by Polδ is remarkably mutagenic.

Polδ (exo-) allows up to 3 nt looping out of template strand

Bypass of 6-4 PP by Polδ (exo-) was associated with slippage event (Fig. 5). We considered three possible mechanisms for the 3-nt looped-out template (Fig. 7A). One is the 6-4 PP-dependent loop formation model, in which highly distorted 6-4 PP promotes 3-nt loop including 6-4 PP (Fig. 7A, upper). The second possible mechanism is sequence-dependent slippage model, in which two consecutive ATG sequence

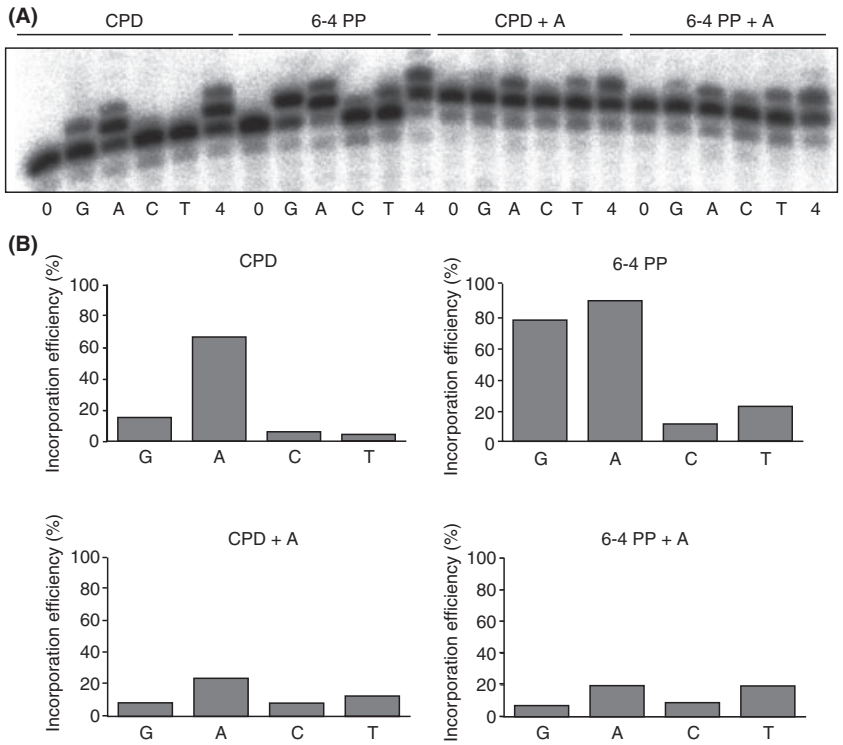

Figure 6 Preference of single nucleotide insertion opposite UV photoproducts. (A) DNA synthesis reactions across CPD or 6-4 PP were carried out with 6 nM Polδ and 8 nM of the primer/template substrate (exo-) in a 5-μL reaction mixture containing each nucleotide separately (10 μM). For the analysis of the first insertion event, a 16mer reverse primer corresponding to 3′ flanking region of T-T dimer, was used (left panel). For the analysis of the second insertion event, a 17mer reverse primer, which has an additional A nucleotide was used (right panel). (B) Quantification of bypass efficiency on damaged templates. The radioactivity was quantified by densitometry, and bypass efficiency was calculated with the following formula: intensity of the elongated product/the total intensity of all bands.

in the 3′ end of the primer strand is looped out, which allows extension by Polδ of an additional copy of ATG before bypassing lesion site. Then, the second slippage occurs such that the most 3′ ATG at the primer end anneals to a CAT 5′ to the lesion (Fig. 7A, middle). The third possible mechanism is the other sequence-dependent loop formation model, in which Polδ first incorporates A opposite 3′ of T-T dimmer, and this nascent A pairs with nondamaged T on the template (Fig. 7A, lower). We wished to verify which of the mechanism underlies slippage event of Polδ and used other three templates, which locates T at 2, 4 and 9 nt upstream from the 3′ T of the lesion site (Figs 1 and 7B,a). If the looping out occurs sequence independently, products from all templates may accompany 3-bp deletion (Fig. 7B). If the sequential looping out and slippage at the ATG repeat in the primer causes 3-bp deletion, products from these three templates may not have deletion, as these templates do not possess CAT 5′ to the lesion. If the looping out is promoted by the third model, these template strands result in 2, 4 and 9 nt looping out (Fig. 7B,b–d). Consistent with the third model, when we used AAT template that allows 2 nt looping out, 2-bp deletion was detected (Fig. 7C). Interestingly, we detected no deletion event, when we used template TAC and AAC, in which 4 and 9 nt looping out was allowed. These results suggest that slippage event of Polδ is highly dependent on the sequence context of template strand and Polδ (exo-) allows up to 3 nt looping out of template strand during bypass of 6-4 PP. More importantly, Polδ (exo-) bypassed 6-4 PP and fully synthesized DNA on all templates carrying 6-4 PP, indicating bypass of 6-4 PP by Polδ (exo-) is not dependent on the sequence context of the template.

Discussion

It is believed that the extraordinarily high accuracy of Polδ is intimately associated with its incapability to

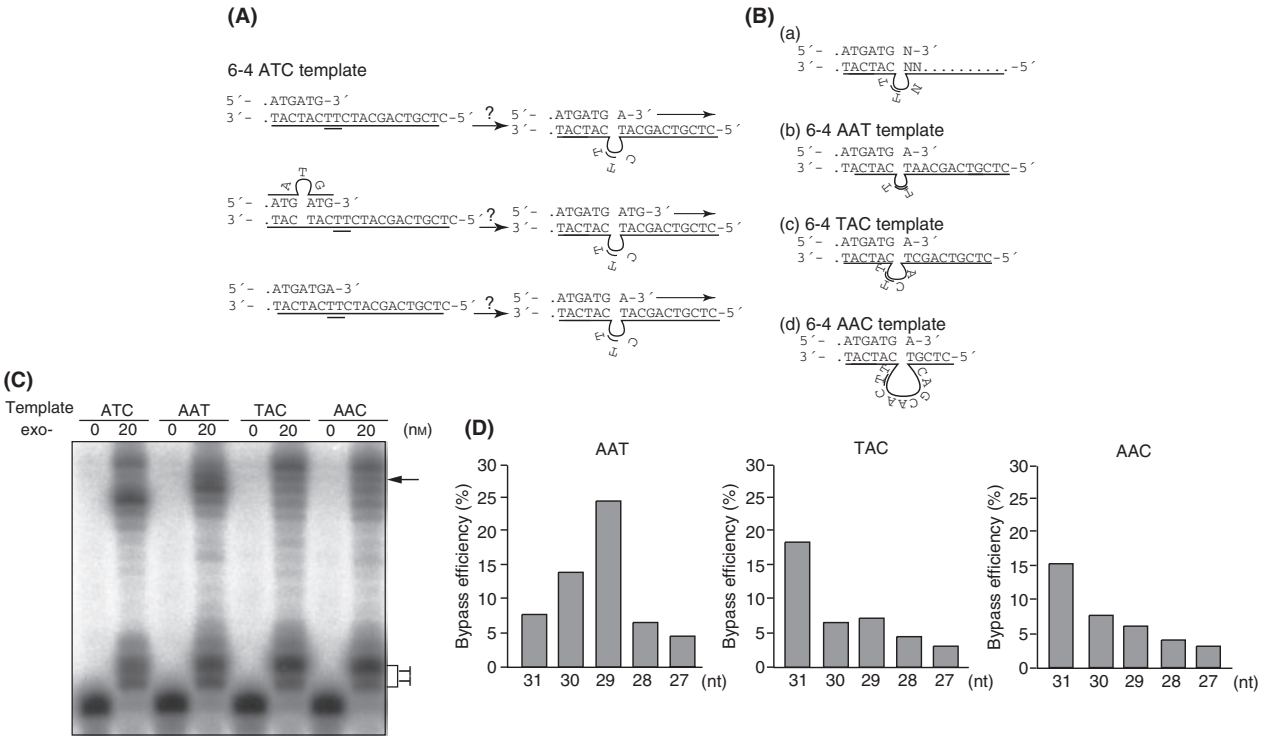

Figure 7 The sequence-dependent looping out mechanism. (A) Three possible looping out mechanisms. (Upper) The 6-4 PP-dependent loop formation model: the 6-4 PP distorts the DNA backbone and promotes 3-nt loop. In this model, the size of the loop should be 3 nt in any template sequence. (Middle) Sequential looping out and slippage at the consecutive ATG in primer model: Two consecutive ATG sequence in the 3′ end of the primer strand is looped out, leading to addition of ATG copy. Then, the second slippage occurs such that the most 3′ ATG at the primer end anneals to a CAT 5′ to the lesion. In this model, 3-bp deletion is dependent on the CAT 5′ to the lesion on the template strand. (Lower) The sequence-dependent loop formation model: Polδ first incorporates A opposite 3′ of T-T dimmer, and this nascent A pairs with nondamaged T on the template. In this model, the size of loop is dependent on the position of T in the template. (B) The loop formation based on each model. (a) According to the 6-4 PP-dependent loop formation model, all three templates should form 3-nt loop. (b–d) In sequence-dependent loop formation model, the sizes of the loops vary depending on the sequences of the template. (C) DNA synthesis reactions using 6-4 PP templates carrying different sequence at 5′ of 6-4 PP. Reactions were carried in the presence of 20 nM Polδ (exo-) and 100 μM dNTP at 37 °C. Parentheses indicate the position of the T-T dimer on the template. The position of the fully elongated product is indicated with an arrow. Note that the top bands indicate 31mer products, which is 1 nucleotide longer than the template. (D) Quantification of bypass efficiency on damaged templates. The radioactivity of each band was quantified by densitometry. Synthesis efficiency was calculated as described in Fig. 5B.

undergo DNA synthesis over damaged nucleotides on the template strand. We show here that Polδ can bypass 6-4 PP, although no other single eukaryotic DNA polymerase can do so (Seki & Wood 2008). The ability of Polδ to bypass 6-4 PP is surprising for the following reasons. First, 6-4 PP causes a pronounced distortion in the DNA backbone and thereby strongly interferes with the Watson–Crick base pairing (Yamamoto *et al.* 2008). Therefore, a nucleotide opposite 6-4 PP on template strands is unlikely to fit in the catalytic core of any DNA polymerase. Second, crystal structure analysis of the yeast Polδ catalytic site showed that the catalytic site of Polδ recognizes a mismatch with extremely high accuracy and can potentially discriminate a mismatch even 4 base pairs away from the error by directly sensing Watson–Crick geometry (Swan *et al.* 2009). Third, no TLS polymerase has been reported to bypass 6-4 PP by itself *in vitro*. In fact, Seki *et al.* reported that the sequential action of Polι and Polθ, but not either polymerase alone, allows for TLS across 6-4 PP (Seki & Wood 2008). For these reasons, the capability of Polδ to carry out TLS across 6-4 PP was totally unexpected.

While we have referred to a dNTP concentration of 10 μM as physiological, the effective concentration of dNTPs at stalled replication forks *in vivo* is almost

certainly higher than this and may increase to 100 μM. Indeed, the dNTP concentration significantly varies depending on the phase of the cell cycle and the cell type, for example, dNTP concentrations increase upto seven times and reach 50 μM in actively cycling cancer cells (Traut 1994). Moreover, ribonucleotide reductase, which catalyzes the *de novo* synthesis of dNTPs, is recruited to damaged DNA sites and may dramatically increase the concentration of dNTPs locally at the site of DNA repair (Niida *et al.* 2010). Furthermore, if the dNTP concentration is increased at stalled replication forks, the enzymatic mode of Polδ may be changed from error-free to error-prone and thereby carry out the bypass of damaged templates efficiently. This view is supported by the fact that an increase in the concentration of dNTPs activates the TLS capability of yeast replicative polymerase and suppresses the sensitivity of a yeast strain that lacks all TLS polymerases to 4-NQ, a UV-mimetic DNA-damaging agent (Sabouri *et al.* 2008). We therefore favor the idea that efficient *in vitro* TLS by Polδ with 100 μM dNTPs might have relevance to *in vivo* DNA synthesis.

The sequence analysis of bypass products showed that 6-4 PP lesion bypass by Polδ (exo-) is accompanied by slippage event. Moreover, we showed that this slippage event is dependent on the sequence context of the template. Polδ first incorporates A opposite the 3′ T of 6-4PP lesion site, which hybridizes with T locating at the upstream from the lesion and thus stabilizes the looped-out structure (Fig. 7A, lower). Our results also indicate that polδ allows looping out up to 3 nucleotides including the 6-4 PP itself during bypasses of 6-4 PP. Therefore, slippage event occurs only when template sequence allows up to 3-bp looping out. This nucleotide slippage reflects a prominent enzymatic property of Polδ, because slippage events occur very frequently at repeated sequences in mismatch repair-deficient cells (Shah *et al.* 2010). *In vitro* DNA synthesis by Polδ is also frequently associated with slippage events, as single- and multibase deletions are observed more frequently in comparison with base substitutions (Fortune *et al.* 2005). This view is substantiated by the recent structural analysis of *Escherichia coli* PolII (the bacterial Polδ homologue), which showed that the cavity-like structure in the catalytic domain of *E. coli* PolII supplies enough room for the looped-out template DNA and thereby allows slippages (Wang & Yang 2009). Similarly, yeast Polδ (Pol3) possesses a cavity-like flexible structure in the catalytic domain (Fig. S4A,B in Supporting Information). The high degree of sequence conservation between human and yeast suggests that human Polδ also possesses the corresponding features to yeast Polδ (Fig. S4C in Supporting Information).

In this study, we showed novel enzymatic property of Polδ in TLS, but the efficiency of bypass across 6-4 PP in the physiological concentration of dNTP is limited even for Polδ (exo-) (approximately 0.5%; Fig. 4). It should be important to address the relevance of this enzymatic property of Polδ *in vivo*.

Experimental procedures

Expression and purification of Polδ (wt) and Polδ (exo-) enzymes

To construct the Polδ (exo-)-mutant gene, point mutations were introduced so as to change Asp to Ala at amino acid residue 402 of p125 by PCR. The primer sequences used in the mutagenesis are 5′-CCAGAACTTCGCCCTTCCGTACC-3′ and 5′-GGTACGGAAGGGCGAAGTTCTGG-3′. Polδ recombinant enzymes with p125 (wt or exo-), p66, p12 and N-terminal His-tagged p50 were expressed, using a pBacPAK9 vector (Clontech) in High Five cells as described previously (Masutani *et al.* 1999b). A His-tagged Polδ complex was prepared from insect cells as described previously (Shikata *et al.* 2001). The concentration and purity of purified proteins were estimated from the intensity of the bands in a Coomassie Blue-stained polyacrylamide gel (Fig. S1 in Supporting Information). p12 subunit was not detectable in a Coomassie Blue staining.

Measurement of exonuclease activity

Various concentrations of Polδ were mixed with 0.5 μM of 5′-labeled 51mer ssDNA 5′-TTTTTTTTTTTTTTTTTTTTTTTTTTTTACGACGTTGTAAAAGGACGGGCCAGT-3′ in 5 μL buffer (30 mM HEPES pH7.5, 7 mM $MgCl_2$, 500 μM DTT, 50 μg/mL BSA and varying concentrations of dNTPs) and incubated for 15 min at 37 °C. The 5-μL reaction mixture was terminated by adding 1 μL of 10× loading buffer (Takara). After the reaction, the products were separated by 7.5% small polyacrylamide gel (7 × 8.5 cm; 7.5% acrylamide, 0.35% bisacrylamide, 0.5× TBE) and transferred to the Biodyne B Nylon Membrane (PALL). After UV fixation, Biotinylated 51mer ssDNA was detected using Chemiluminescent Nucleic Acid Detection Module (Thermo scientific) according to the manufacturer's instructions.

Primer extension analysis

A concentration of 0.06 pmol of 5′ ^{32}P-labeled 16mer primer 5′-CACTGACTGTATGATG-3′ was annealed to 0.04 pmol of 30mer oligonucleotide template DNA 5′-CTCGTCAGC ATCTTCATCATACAGTCAGTG-3′ (underlined nucleotides indicate the position of TT UV photoproduct for damaged template) and incubated for 15 min in a 5-μL reaction

mixture containing 30 mM HEPES–NaOH (pH 7.4), 7 mM $MgCl_2$, 8 mM NaCl, 0.5 mM dithiothreitol and 10 or 100 μM dNTPs at 37 °C, in the presence of 100 nM PCNA and 2, 6 or 20 nM Polδ. The reaction was terminated by adding 5 μL of 2× formamide dye (98% deionized formamide, 10 mM EDTA, 0.025% xylene cyanol, 0.025% BPB). The denatured products were loaded onto 15.6% polyacrylamide gels containing 7 M urea in TBE buffer (89 mM Tris, 89 mM boric acid, 2 mM EDTA). After electrophoresis, radioactivity was measured with a Fuji Image analyzer, FLA2500 (Fujifilm). In the time-course analysis, the reaction was performed in 50-μL scale, and in each time point, 5 μL of reactant was mixed with 2× formamide dye to terminate reaction.

Sequence analysis of the fully elongated products

A concentration of 0.12 pmol of 5′ biotin-labeled primer was annealed to 30mer templates and used in a primer extension reaction. Each template was assayed in a reaction containing 100 μM dNTPs and 20 nM Polδ (exo-). The extended products were purified by DYNABEADS M-280 STREPTAVIDIN (DYNAL) according to the manufacturer's instructions. Six femtomol of the purified primers was polyadenylated using terminal deoxynucleotidyl transferase (TdT) and 0.25 mM dATP. After PCR amplification using the forward primer (5′-CACTGACTGTATGATG-3′) and reverse primer (5′-TT TTTTTTTTTTTTTTTTTT-3′), the products were cloned to PCR-TOPO vector (Invitrogen) and sequenced using the M13 primer.

Acknowledgements

We thank the members of the Tsurimoto laboratory in Kyushu University for their kind help and technical assistance. This work was supported in part by grants-in-aid for scientific research in a priority area from the Ministry of Education, Culture, Sports, Science and Technology, Japan (to S.T. and K.H.), and grants from the Fujiwara Foundation of Science, the Uehara Memorial Foundation and the Naito Foundation (to K.H.).

References

Blank, A., Kim, B. & Loeb, L.A. (1994) DNA polymerase delta is required for base excision repair of DNA methylation damage in Saccharomyces cerevisiae. *Proc. Natl. Acad. Sci. USA* **91**, 9047–9051.

Brutlag, D. & Kornberg, A. (1972) Enzymatic synthesis of deoxyribonucleic acid. 36. A proofreading function for the 3′ leads to 5′ exonuclease activity in deoxyribonucleic acid polymerases. *J. Biol. Chem.* **247**, 241–248.

Burgers, P.M. (1998) Eukaryotic DNA polymerases in DNA replication and DNA repair. *Chromosoma* **107**, 218–227.

Burgers, P.M. (2009) Polymerase dynamics at the eukaryotic DNA replication fork. *J. Biol. Chem.* **284**, 4041–4045.

Clark, J.M. (1988) Novel non-templated nucleotide addition reactions catalyzed by procaryotic and eucaryotic DNA polymerases. *Nucleic Acids Res.* **16**, 9677–9686.

Edmunds, C.E., Simpson, L.J. & Sale, J.E. (2008) PCNA ubiquitination and REV1 define temporally distinct mechanisms for controlling translesion synthesis in the avian cell line DT40. *Mol. Cell* **30**, 519–529.

Fazlieva, R., Spittle, C.S., Morrissey, D., Hayashi, H., Yan, H. & Matsumoto, Y. (2009) Proofreading exonuclease activity of human DNA polymerase delta and its effects on lesion-bypass DNA synthesis. *Nucleic Acids Res.* **37**, 2854–2866.

Fortune, J.M., Pavlov, Y.I., Welch, C.M., Johansson, E., Burgers, P.M. & Kunkel, T.A. (2005) *Saccharomyces cerevisiae* DNA polymerase delta: high fidelity for base substitutions but lower fidelity for single- and multi-base deletions. *J. Biol. Chem.* **280**, 29980–29987.

Friedberg, E.C., Lehmann, A.R. & Fuchs, R.P. (2005) Trading places: how do DNA polymerases switch during translesion DNA synthesis? *Mol. Cell* **18**, 499–505.

Guo, C., Kosarek-Stancel, J.N., Tang, T.S. & Friedberg, E.C. (2009) Y-family DNA polymerases in mammalian cells. *Cell. Mol. Life Sci.* **66**, 2363–2381.

Guo, C., Tang, T.S., Bienko, M., Dikic, I. & Friedberg, E.C. (2008) Requirements for the interaction of mouse Polkappa with ubiquitin and its biological significance. *J. Biol. Chem.* **283**, 4658–4664.

Jamburuthugoda, V.K., Chugh, P. & Kim, B. (2006) Modification of human immunodeficiency virus type 1 reverse transcriptase to target cells with elevated cellular dNTP concentrations. *J. Biol. Chem.* **281**, 13388–13395.

Kim, J.K. & Choi, B.S. (1995) The solution structure of DNA duplex-decamer containing the (6-4) photoproduct of thymidylyl(3′–>5′)thymidine by NMR and relaxation matrix refinement. *Eur. J. Biochem.* **228**, 849–854.

Kunkel, T.A. & Burgers, P.M. (2008) Dividing the workload at a eukaryotic replication fork. *Trends Cell Biol.* **18**, 521–527.

Lehmann, A.R., Niimi, A., Ogi, T., Brown, S., Sabbioneda, S., Wing, J.F., Kannouche, P.L. & Green, C.M. (2007) Translesion synthesis: Y-family polymerases and the polymerase switch. *DNA Repair (Amst)* **6**, 891–899.

Ling, H., Boudsocq, F., Woodgate, R. & Yang, W. (2001) Crystal structure of a Y-family DNA polymerase in action: a mechanism for error-prone and lesion-bypass replication. *Cell* **107**, 91–102.

Masutani, C., Araki, M., Yamada, A., Kusumoto, R., Nogimori, T., Maekawa, T., Iwai, S. & Hanaoka, F. (1999a) Xeroderma pigmentosum variant (XP-V) correcting protein from HeLa cells has a thymine dimer bypass DNA polymerase activity. *EMBO J.* **18**, 3491–3501.

Masutani, C., Kusumoto, R., Iwai, S. & Hanaoka, F. (2000) Mechanisms of accurate translesion synthesis by human DNA polymerase eta. *EMBO J.* **19**, 3100–3109.

Masutani, C., Kusumoto, R., Yamada, A., Dohmae, N., Yokoi, M., Yuasa, M., Araki, M., Iwai, S., Takio, K. & Hanaoka, F. (1999b) The XPV (xeroderma pigmentosum variant) gene encodes human DNA polymerase eta. *Nature* **399**, 700–704.

McCulloch, S.D., Kokoska, R.J., Masutani, C., Iwai, S., Hanaoka, F. & Kunkel, T.A. (2004) Preferential cis-syn thymine dimer bypass by DNA polymerase eta occurs with biased fidelity. *Nature* **428**, 97–100.

Meng, X., Zhou, Y., Zhang, S., Lee, E.Y., Frick, D.N. & Lee, M.Y. (2009) DNA damage alters DNA polymerase delta to a form that exhibits increased discrimination against modified template bases and mismatched primers. *Nucleic Acids Res.* **37**, 647–657.

Nick McElhinny, S.A., Gordenin, D.A., Stith, C.M., Burgers, P.M. & Kunkel, T.A. (2008) Division of labor at the eukaryotic replication fork. *Mol. Cell* **30**, 137–144.

Niida, H., Katsuno, Y., Sengoku, M., Shimada, M., Yukawa, M., Ikura, M., Ikura, T., Kohno, K., Shima, H., Suzuki, H., Tashiro, S. & Nakanishi, M. (2010) Essential role of Tip60-dependent recruitment of ribonucleotide reductase at DNA damage sites in DNA repair during G1 phase. *Genes Dev.* **24**, 333–338.

Niimi, A., Brown, S., Sabbioneda, S., Kannouche, P.L., Scott, A., Yasui, A., Green, C.M. & Lehmann, A.R. (2008) Regulation of proliferating cell nuclear antigen ubiquitination in mammalian cells. *Proc. Natl Acad. Sci. USA* **105**, 16125–16130.

Podust, V.N., Chang, L.S., Ott, R., Dianov, G.L. & Fanning, E. (2002) Reconstitution of human DNA polymerase delta using recombinant baculoviruses: the p12 subunit potentiates DNA polymerizing activity of the four-subunit enzyme. *J. Biol. Chem.* **277**, 3894–3901.

Prakash, L. (1981) Characterization of postreplication repair in *Saccharomyces cerevisiae* and effects of *rad6*, *rad18*, *rev3* and *rad52* mutations. *Mol. Gen. Genet.* **184**, 471–478.

Sabouri, N., Viberg, J., Goyal, D.K., Johansson, E. & Chabes, A. (2008) Evidence for lesion bypass by yeast replicative DNA polymerases during DNA damage. *Nucleic Acids Res.* **36**, 5660–5667.

Seki, M. & Wood, R.D. (2008) DNA polymerase theta (POLQ) can extend from mismatches and from bases opposite a (6-4) photoproduct. *DNA Repair (Amst)* **7**, 119–127.

Shah, S.N., Hile, S.E. & Eckert, K.A. (2010) Defective mismatch repair, microsatellite mutation bias, and variability in clinical cancer phenotypes. *Cancer Res.* **70**, 431–435.

Shikata, K., Ohta, S., Yamada, K., Obuse, C., Yoshikawa, H. & Tsurimoto, T. (2001) The human homologue of fission Yeast cdc27, p66, is a component of active human DNA polymerase delta. *J. Biochem.* **129**, 699–708.

Silvian, L.F., Toth, E.A., Pham, P., Goodman, M.F. & Ellenberger, T. (2001) Crystal structure of a DinB family error-prone DNA polymerase from Sulfolobus solfataricus. *Nat. Struct. Biol.* **8**, 984–989.

Swan, M.K., Johnson, R.E., Prakash, L., Prakash, S. & Aggarwal, A.K. (2009) Structural basis of high-fidelity DNA synthesis by yeast DNA polymerase delta. *Nat. Struct. Mol. Biol.* **16**, 979–986.

Tissier, A., Frank, E.G., McDonald, J.P., Iwai, S., Hanaoka, F. & Woodgate, R. (2000) Misinsertion and bypass of thymine–thymine dimers by human DNA polymerase iota. *EMBO J.* **19**, 5259–5266.

Traut, T.W. (1994) Physiological concentrations of purines and pyrimidines. *Mol. Cell. Biochem.* **140**, 1–22.

Trincao, J., Johnson, R.E., Escalante, C.R., Prakash, S., Prakash, L. & Aggarwal, A.K. (2001) Structure of the catalytic core of *S. cerevisiae* DNA polymerase eta: implications for translesion DNA synthesis. *Mol. Cell* **8**, 417–426.

Wang, F. & Yang, W. (2009) Structural insight into translesion synthesis by DNA Pol II. *Cell* **139**, 1279–1289.

Waters, L.S., Minesinger, B.K., Wiltrout, M.E., D'Souza, S., Woodruff, R.V. & Walker, G.C. (2009) Eukaryotic translesion polymerases and their roles and regulation in DNA damage tolerance. *Microbiol. Mol. Biol. Rev.* **73**, 134–154.

Yamamoto, J., Loakes, D., Masutani, C., Simmyo, S., Urabe, K., Hanaoka, F., Holliger, P. & Iwai, S. (2008) Translesion synthesis across the (6-4) photoproduct and its Dewar valence isomer by the Y-family and engineered DNA polymerases. *Nucleic Acids Symp. Ser. (Oxf)* **52**, 339–340.

Yang, W. (2005) Portraits of a Y-family DNA polymerase. *FEBS Lett.* **579**, 868–872.

Received: 3 June 2010
Accepted: 8 September 2010

Supporting Information/Supplementary material

The following Supporting Information can be found in the online version of the article:

Figure S1 Purification profile of Polδ.

Figure S2 Primer extension by Polδ holoenzyme on abasic site-containing templates.

Figure S3 Sequence alignment data of the primer extended products in Fig. 5.

Figure S4 Sequence and structure comparison between Polδ homologues.

Additional Supporting Information may be found in the online version of this article.

Please note: Wiley-Blackwell are not responsible for the content or functionality of any supporting materials supplied by the authors. Any queries (other than missing material) should be directed to the corresponding author for the article.